

# Fabrication of Gd<sub>2</sub>O<sub>3</sub>/PSF Membranes via Aqueous Phase Inversion Method

Ayşe Gul<sup>1</sup>  Dilek Senol Arslan<sup>2</sup>  Nigmet Uzal<sup>1</sup> 

<sup>1</sup>Abdullah Gul University, Department of Civil Engineering, Kayseri, Turkey

<sup>2</sup>Abdullah Gul University, Department of Nanotechnology Engineering, Kayseri, Turkey

## ABSTRACT

The purpose of this study was to look into the effect of Gadolinium oxide (Gd<sub>2</sub>O<sub>3</sub>) concentration (0.5%, 1%, and 2%) on the performance of newly developed Gd<sub>2</sub>O<sub>3</sub>/PSF membranes. A common phase inversion method was used to create the membranes. Pure water flux and bovine serum albumin (BSA) permeation tests were used to evaluate membrane performance. FTIR and contact angle measurements were used to characterize the membranes that were manufactured. The greatest percentage of BSA rejection was 53%. In this work, the optimum membrane (2% wt Gd<sub>2</sub>O<sub>3</sub>/17% wt PSF) successfully demonstrated 53% rejection with filtrate flux for about 8.7 L/m<sup>2</sup>.h at a pressure of 10 bar.

### Keywords:

Gadolinium oxide (Gd<sub>2</sub>O<sub>3</sub>); Polysulfone (PSF); Membrane; Bovine serum albumin; Phase inversion method.

### Article History:

Received: 2022/06/08

Accepted: 2022/08/18

Online: 2022/09/28

### Correspondence to:

Dilek Senol Arslan  
Department of Nanotechnology  
Engineering, Abdullah Gül University,  
38380 Kayseri, Turkey  
Tel: +90 539 799 39 00  
E-Mail:dilek.senol@agu.edu.tr

## INTRODUCTION

Membrane technology, especially microfiltration (MF) and ultrafiltration (UF) membranes is rapidly being employed in separation processes due to benefits such as 100% particle removal, reduced chemical usage, and a compact footprint, as well as financial, environmental, and safety advantages. Membrane characteristics have been adapted and altered to the specific job to date in order to benefit from a wide range of industrial applications, including the separation and purification of protein molecules [1-3].

The most prevalent protein in blood plasma, bovine serum albumin (BSA), is one of the most researched proteins in the serum albumin family. In terms of its role in the pharmaceutical and food industry, the separation of Bovine serum albumin (BSA) is one of the most important proteins that require membranes with high permeability and selectivity [4].

Gadolinium (Gd), is a member of the lanthanide family of elements that is mostly employed in the medical field as contrast and anti-cancer agent for Magnetic Resonance Imaging (MRI) and medication administration, as well as in the nuclear power industry [5, 6]. Due to its excellent properties and characteristics, such as mechanical strength, chemical and structural stability, and thermal resistance, polysulfone (PSF) is preferred as a membrane polymer for use in purification [7].

Some researchers examined the performance of a Gadolinium-based composite membrane for dye and arsenic removal from water. Zhao et al. recently completed a study employing gadolinium doped cobalt ferrite nanoparticles to remove Congo red [8]. Another recent work used Fe<sub>3</sub>O<sub>4</sub>-GO-Gd<sub>2</sub>O<sub>3</sub> to treat polluted water and found that the poor adsorption capacity of 35.85 mg/g was attributable to material aggregation [9].

In this study, the performance of PSF and PSF/Gd<sub>2</sub>O<sub>3</sub> membranes for BSA separation was investigated.

## MATERIALS AND METHODS

### Materials

The chemicals used in this work were PSF (with average Mw = 60,000 Da) was used as the polymer in the dope solution (Acros Organics). N,N Dimethylformamide was used as a solvent to prepare membrane cast solution (ISOLAB chemicals). Gadolinium oxide (Gd<sub>2</sub>O<sub>3</sub>) powder (99%, hydrophilic) was purchased from Nanografi A.Ş., Turkey. Ultra-pure water with 18.2 MΩ cm resistivity was used all experimental procedures. As a contaminant, bovine serum albumin (BSA) was used all experiments (Amresco Inc., USA).

## Methods

### Membrane fabrication

The Gd<sub>2</sub>O<sub>3</sub>/PSF membranes were fabricated by the typical phase inversion method. The casting solution consist of PSF; 17 wt % and 3 different concentrations of Gd<sub>2</sub>O<sub>3</sub> (0.5 wt %, 1 wt % and 2 wt %) were dissolved in NMP. The solution was stirred for 24 h at 500 rpm around 20°C. Then, the solution was sonicated for 10 min for the exit of the air bubble. A schematic representation of the fabrication of Gd<sub>2</sub>O<sub>3</sub>/PSF membrane and dynamic membrane filtration process is presented in Fig. 1.

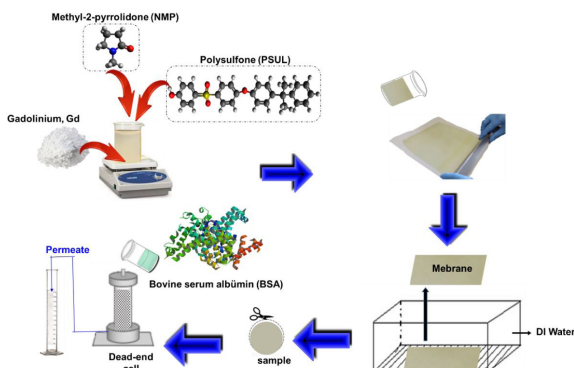


**Figure 1.** Schematic representation of the fabrication of PSF- Gd<sub>2</sub>O<sub>3</sub> membrane and dynamic membrane filtration process.

### Bovine Serum Albumin rejection experiments

In the dead-end filtration module, the membranes bovine serum albumin (BSA) rejection performance was examined using aqueous solutions with the initial concentration of 2.5 g/L of BSA at 10 bar TMP. Deionized water (DI) was used to prepare the solutions, which were kept at room temperature. A UV spectrophotometer was used to determine the concentration of BSA solution in the filtrate at a wavelength of 278.5 nm. The rejection rate of the membrane was defined by Eq. 1.

$$R = \frac{C_1 - C_2}{C_1} \times 100\% \quad (1)$$

where R is the membrane rejection rate (%), C<sub>1</sub> is initial concentration of BSA in the permeate (g/L), C<sub>2</sub> is the BSA concentration in the feed solution filtrate (g/L).

### Pure water flux

Water filtration experiments were performed in a dead-end stirred cell filtration system (Sterlitech, HP4750). The dead-end filtration system has a membrane surface area of 14.6 cm<sup>2</sup> and a volume capacity of 300 mL. The membranes that had been tested, PSF and PSF/ Gd<sub>2</sub>O<sub>3</sub>, were placed in the filtration cell, which was then filled with 250 ml of clean water. A nitrogen gas cylinder was connected to the membrane filtration cell. DI water was used in all experiments.

In the pure water flux experiments at a constant trans-membrane pressure (TMP) of 10 bar at room temperature (25°C). The pure water flux was measured every 15 minutes. Eq. 2 was used to calculate the water fluxes of the PSF and PSF/Gd<sub>2</sub>O<sub>3</sub> membranes.

$$J = V / (A \times \Delta t) \quad (2)$$

where J is the water flux (L/m<sup>2</sup>h), V is the volume of permeate (L), Δt is time (h) and A is the effective membrane area (m<sup>2</sup>).

## RESULTS AND DISCUSSION

The zeta potential-pH behavior was characterized using a Nano ZS90 (Malvern, UK) equipment. 0.5 g Gd<sub>2</sub>O<sub>3</sub> nanoparticles were conditioned in 50 mL of DI water for 30 min (1% solid ratio). The pH of the solution was adjusted by using 0.1 mol/L H<sub>2</sub>SO<sub>4</sub> and 0.1 mol/L NaOH, and the solution was kept for 20 min to let the bigger particles settle.

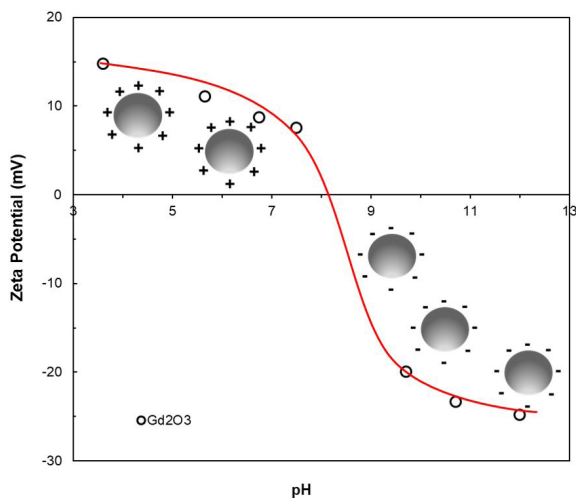


**Figure 2.** Zeta potential of Gd<sub>2</sub>O<sub>3</sub> nanoparticles.

Fig.2 shows the pH dependence of the zeta potential of Gd<sub>2</sub>O<sub>3</sub> nanoparticles. The isoelectric point (iep) was determined 8.1. Above the iep value, the Gd<sub>2</sub>O<sub>3</sub> surface is negatively charged, while below the iep value the Gd<sub>2</sub>O<sub>3</sub> surface is positively charged.

### SEM analysis

The surface morphologies of the Gd<sub>2</sub>O<sub>3</sub> powder and Ni-Zn MOF embedded membranes were assessed using a scanning electron microscope (Zeiss Gemini) with an app-

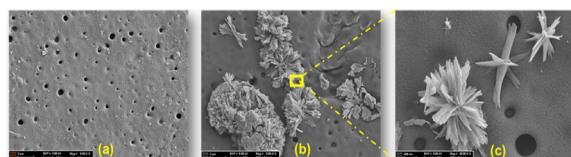


**Figure 3.** Schematic illustration showing the Scanning electron microscopic images of (a) PSF membrane, (b) Gd<sub>2</sub>O<sub>3</sub>/PSF membrane, and high-magnification of flower shape.

lied voltage of 10 kV. SEM images of the samples were given in Fig. 3.

As can be seen in Fig.3, the pure PSF membrane showed a clean and porous surface (Fig. 3a). The  $Gd_2O_3$ /PSF membrane (2 wt %) showed a porous surface with  $Gd_2O_3$  particles (Fig. 3b). Some  $Gd_2O_3$  nanoparticles formed aggregates embedded on the surface within the pores of the membrane (Fig. 3c).

### FT-IR measurements

All FT-IR measurements were performed with an FT-IR spectrometer (Thermo Nicolet Avatar 370) for functional identification of PSF and embedded PSF membranes. The surface hydrophilicity of the  $Gd_2O_3$  powder embedded in 3 different membranes was measured by a contact angle meter (Attention-Theta Lite, Biolin Scientific, Finland) with the sessile drop method.

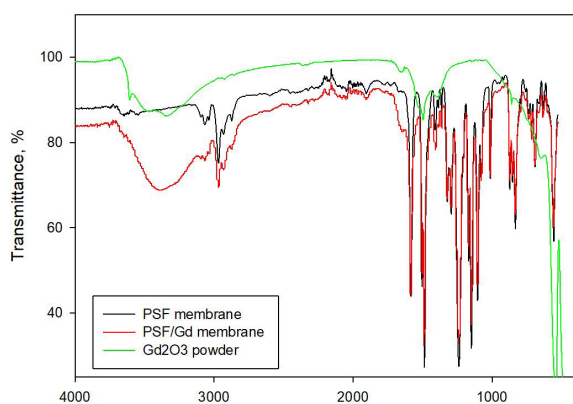


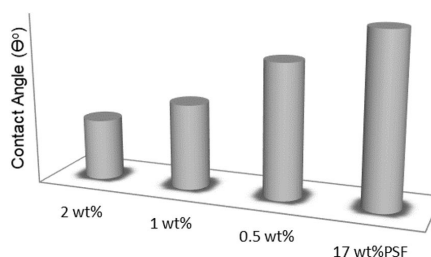
**Figure 4.** FT-IR spectra of PSF membrane and  $Gd_2O_3$ /PSF membrane and  $Gd_2O_3$  powder.

Two spectra for PSF membrane and PSF/  $Gd_2O_3$  membrane were recorded in the region 400–4000 $cm^{-1}$ .

The peak at 1487  $cm^{-1}$  and 1584  $cm^{-1}$  which corresponds to an aromatic vibrational bonding of C=C in the polysulfone group [10]. OH stretching vibrations at 3646  $cm^{-1}$  attributed to inner surface hydroxyl stretching [11]. For the  $Gd_2O_3$ /PSF membrane, the broadband at 3100–3500  $cm^{-1}$  is attributed to O-H stretch [12]. As shown in Fig. 4, the new peaks at 470  $cm^{-1}$  and 541  $cm^{-1}$  assigned to the Gd–O vibration of  $Gd_2O_3$ . It shows that  $Gd_2O_3$  particles are successfully incorporated into the PSF membrane. Therefore, the presence of  $Gd_2O_3$  is the reason why the membrane becomes hydrophilic. Similar findings have previously been reported by [13, 14].

### Membrane hydrophilicity

The hydrophobic or hydrophilic characteristics on the flat membrane surfaces (PSF and PSF/  $Gd_2O_3$  membranes (0.5 wt %  $Gd_2O_3$ , 1 wt %  $Gd_2O_3$ , and 2 wt %  $Gd_2O_3$ ) were determined by contact angle measurements.



Contact angle	2 wt%	1 wt%	0.5 wt%	17 wt%PSF
Contact angle	74 ± 2	76 ± 4	80 ± 2	83 ± 3

**Figure 5.** Contact angles of PSF membrane and PSF/  $Gd_2O_3$  membranes (0.5 wt %  $Gd_2O_3$ , 1 wt %  $Gd_2O_3$ , and 2 wt %  $Gd_2O_3$ )

As can be seen in Fig.5., a significant decrease in the contact angle of water drops from 83±3° for the PSF membrane surface to 9±2.5° for the surface of 2 wt %  $Gd_2O_3$  embedded PSF membrane. This decrease of contact angle revealed Gd's hydrophilic property, which is clarified by the presence of the polar -OH groups on the Gadolinium(III) hydroxide hydrate surface [15].

### Water filtration and rejection of BSA experiments

The capacity of the membrane to filter solutions, also known as flux or permeability, is a key metric for its performance. Another critical parameter is the membrane's capacity to remove components or particles from the solution, typically known as solute rejection [16].

Pure water filtration tests were performed on PSF membranes with three varied concentrations of  $Gd_2O_3$  concentration (0.5wt %, 1 wt %, and 2wt %) to determine their permeability.

The pure water fluxes of PSF, 0.5 wt %  $Gd_2O_3$ , 1 wt %  $Gd_2O_3$ , and 2 wt %  $Gd_2O_3$  were determined at 10 bar using a dead-end filtration system, and the results are shown in Fig. 6, where the pure water fluxes of 17 wt % wt PSE, 0.5 wt %  $Gd_2O_3$ , 1 wt %  $Gd_2O_3$ , and 2 wt %  $Gd_2O_3$  are 81.6, 8.5, 14.3 and 18.1 L m<sup>-2</sup> h<sup>-1</sup>, respectively.

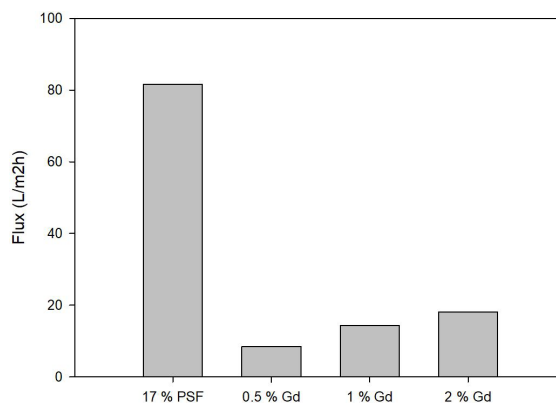


**Figure 6.** Pure water flux of 17 wt % PSF; 0.5 wt %  $Gd_2O_3$ , 1 wt %  $Gd_2O_3$ , and 2 wt %  $Gd_2O_3$  membrane.

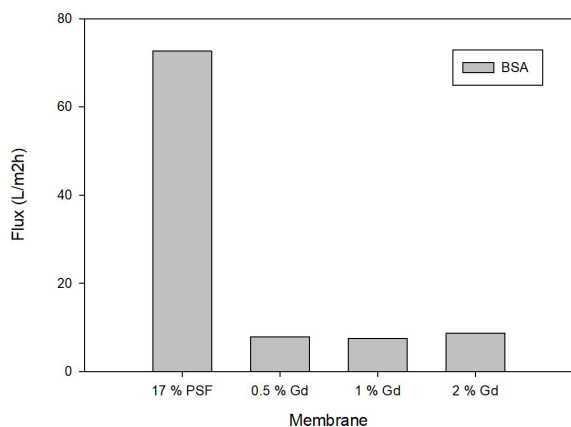


**Figure 7.** BSA flux of 17 wt % PSF; 0.5 wt % Gd<sub>2</sub>O<sub>3</sub>, 1 wt % Gd<sub>2</sub>O<sub>3</sub>, and 2 wt % Gd<sub>2</sub>O<sub>3</sub> membrane.

The membranes BSA rejection performance was investigated in the dead-end filtration module using aqueous solutions with an initial concentration of 2.5 g/L of BSA at 10 bar TMP. BSA flux and BSA rejection values of prepared PSF and PSF/Gd<sub>2</sub>O<sub>3</sub> membranes are given in Figs 7-9.

The permeability of BSA was measured when the pure water was replaced with a BSA solution, and the flux of these membranes significantly reduced as shown in Fig 5 where the BSA fluxes of 17 wt% PSF, 0.5 wt % Gd<sub>2</sub>O<sub>3</sub>, 1 wt% Gd<sub>2</sub>O<sub>3</sub>, and 2 wt % Gd<sub>2</sub>O<sub>3</sub> are 72.6, 7.9, 7.5 and 8.7 L m<sup>-2</sup> h<sup>-1</sup>, respectively.

The flux differences are explained by the fact that as the membrane surface becomes rough and the pore structure inside the membrane becomes more complicated, the membrane pores become blocked, decreasing BSA flux [17]. The adsorption or deposition of protein molecules inside the membrane pores, which causes antifouling activity within the membranes by the partial blocking of membrane pores, is responsible for the decrease in water flux of BSA aqueous solution [18].

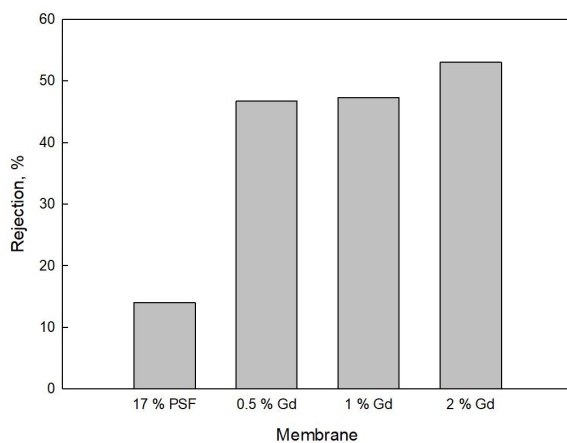


**Figure 8.** The BSA rejection for prepared membranes (17 wt % PSF; 0.5 wt % Gd<sub>2</sub>O<sub>3</sub>, 1 wt % Gd<sub>2</sub>O<sub>3</sub>, and 2 wt % Gd<sub>2</sub>O<sub>3</sub>).

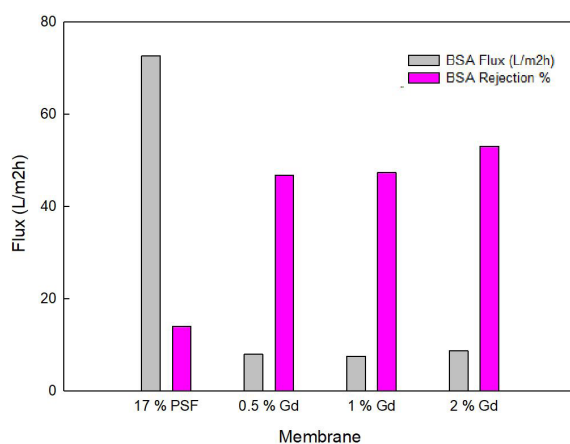


**Figure 9.** The BSA rejection for prepared membranes (17 wt % PSF; 0.5

PSF and PSF/Gd BSA rejection values ranged from 14% to 53%. PSF/ Gd<sub>2</sub>O<sub>3</sub> membranes were shown to reject more than 45% of the BSA, with the PSF 2 wt % Gd<sub>2</sub>O<sub>3</sub> nanocomposite membrane showing the highest BSA rejection at 53%.

Fluxes and rejection of BSA solutions were measured and the results were shown in Fig. 9. The increased concentration of Gd<sub>2</sub>O<sub>3</sub> in the membranes was evaluated using BSA flux and BSA rejection ratio. Rejection of BSA increased when BSA flux decreased. Many variables affect membrane permeability, including membrane shape, surface roughness, surface pore size, and surface hydrophilicity.

## CONCLUSION

The present study examines the rejection of BSA with a newly developed Gd<sub>2</sub>O<sub>3</sub>/PSF membranes. The following conclusions can be drawn;

- BSA rejection increased with increasing Gd<sub>2</sub>O<sub>3</sub> concentration. Therefore, this is also enhanced the Gd<sub>2</sub>O<sub>3</sub>/PSF membrane separation performance.
- FT-IR spectra suggest the presence of chemical bonding with Gd<sub>2</sub>O<sub>3</sub> and functional groups.
- A significant decrease in the contact angle of water drops from 83±3° for the PSF membrane surface to 9±2.5° for the surface of 2wt % Gd<sub>2</sub>O<sub>3</sub> embedded PSF membrane.
- PSF/Gd<sub>2</sub>O<sub>3</sub> membranes showed better BSA rejection than pure PSF membrane.
- The highest BSA rejection efficiency was observed with 2 wt % Gd<sub>2</sub>O<sub>3</sub>, at pH 8.

## CONFLICT OF INTEREST

Authors approve that to the best of their knowledge, there is not any conflict of interest or common interest with an institution/organization or a person that may affect the review process of the paper.

## AUTHOR CONTRIBUTION

All authors contributed to the study conception and design. Material preparation, data collection and analysis

were performed by Ayse Gul, Dilek Senol-Arslan and Nigmat Uzal. The first draft of the manuscript was written by Dilek Senol-Arslan and all authors commented on previous versions of the manuscript. All authors read and approved the final manuscript.

## REFERENCES

1. Monash, P., A. Majhi, and G. Pugazhenth, Separation of bovine serum albumin (BSA) using  $\gamma$ -Al<sub>2</sub>O<sub>3</sub>-clay composite ultrafiltration membrane. *Journal of Chemical Technology & Biotechnology*, 2010. 85(4): p. 545-554.
2. Alia, N.a., et al., Preparation and characterization of a polysulfone ultrafiltration membrane for bovine serum albumin separation: Effect of polymer concentration. *Desalination and water treatment*, 2011. 32(1-3): p. 248-255.
3. Hashino, M., et al., Effect of kinds of membrane materials on membrane fouling with BSA. *Journal of Membrane Science*, 2011. 384(1-2): p. 157-165.
4. Fahrina, A., et al., Development of anti-microbial polyvinylidene fluoride (PVDF) membrane using bio-based ginger extract-silica nanoparticles (GE-SiNPs) for bovine serum albumin (BSA) filtration. *Journal of the Taiwan Institute of Chemical Engineers*, 2021. 125: p. 323-331.
5. Davoodi-Nasab, P., et al., Evaluation of the emulsion liquid membrane performance on the removal of gadolinium from acidic solutions. *Journal of Molecular Liquids*, 2018. 262: p. 97-103.
6. Unruh, C., et al., Benefits and detriments of gadolinium from medical advances to health and ecological risks. *Molecules*, 2020. 25(23): p. 5762.
7. Saki, S. and N. Uzal, Preparation and characterization of PSF/PEI/CaCO<sub>3</sub> nanocomposite membranes for oil/water separation. *Environmental Science and Pollution Research*, 2018. 25(25): p. 25315-25326.
8. Zhao, X., et al., Synthesis and characterization of gadolinium doped cobalt ferrite nanoparticles with enhanced adsorption capability for Congo Red. *Chemical Engineering Journal*, 2014. 250: p. 164-174.
9. Choi, J.-S., et al., Fabrication of chitosan/graphene oxide-gadolinium nanorods as a novel nanocomposite for arsenic removal from aqueous solutions. *Journal of Molecular Liquids*, 2020. 320: p. 114410.
10. Nasirian, D., et al., Investigation of the gas permeability properties from polysulfone/polyethylene glycol composite membrane. *Polymer Bulletin*, 2020. 77(10): p. 5529-5552.
11. Nandiyanto, A.B.D., R. Oktiani, and R. Ragadhita, How to read and interpret FTIR spectroscopy of organic material. *Indonesian Journal of Science and Technology*, 2019. 4(1): p. 97-118.
12. Riyahi-Alam, S., et al., Size reproducibility of gadolinium oxide based nanomagnetic particles for cellular magnetic resonance imaging: effects of functionalization, chemisorption and reaction conditions. *Iranian journal of pharmaceutical research: IJPR*, 2015. 14(1): p. 3.
13. Yousefi, T., et al., Synthesis of Gd<sub>2</sub>O<sub>3</sub> nanoparticles: using bulk Gd<sub>2</sub>O<sub>3</sub> powders as precursor. *Rare Metals*, 2015. 34(8): p. 540-545.
14. Whba, F., et al., The crystalline structure of gadolinium oxide nanoparticles (Gd<sub>2</sub>O<sub>3</sub>-NPs) synthesized at different temperatures via X-ray diffraction (XRD) technique. *Radiation Physics and Chemistry*, 2021. 179: p. 109212.
15. Touzi, H., et al., Detection of Gadolinium with an Impedimetric Platform Based on Gold Electrodes Functionalized by 2-Methylpyridine-Substituted Cyclam. *Sensors*, 2021. 21(5): p. 1658.
16. Razi F, M.S.a.A.N., The performance of bovine serum albumin filtration by using polyethersulfone-Tetronic 304 blend Ultrafiltration Membrane F1000Research 2019.
17. Wang, Q., et al., High rejection performance ultrafiltration membrane with ultrathin dense layer fabricated by the movement and dissolution of metal-organic frameworks. *New Journal of Chemistry*, 2020. 44(32): p. 13745-13754.
18. Ahmad, S., W.A. Siddiqi, and S. Ahmad, Facile hydrophilic chitosan and graphene oxide modified sustainable non-woven fabric composite sieve membranes (NWF@ Cs/Gx): Antifouling, protein rejection, and oil-water emulsion separation studies. *Chemical Engineering Research and Design*, 2022. 181: p. 220-238.